PAPER

Check for updates

Target-selective cytosolic delivery of cargo proteins using the VHH-presented OLE-ZIP capsules†

Kousuke Takahashi,[a] Yasumichi Inoue,[b] Shigeaki Hida,[b] Ryuki Hosoda,[a] Naoki Umezawa, [ID][b] Isamu Akiba, [ID][c] Mitsuo Umetsu [ID][d] and Toshihisa Mizuno [ID] *[a,e]

In the pursuit of a new generation of protein pharmaceuticals, the efficient delivery of these therapeutics into cells stands out as a crucial challenge. In this study, we have developed a novel approach utilizing protein capsules modified with VHH antibodies as cytosolic carriers for protein pharmaceuticals. For the protein capsule component, we opted for the OLE-ZIP protein capsules, which can be prepared from the amphiphilic two-helix bundled protein OLE-ZIP using the water-in-oil (w/o) emulsion method. The spacious interior of the OLE-ZIP capsules allows for the stable encapsulation of over 200 molecules of protein pharmaceuticals, such as RNase A and Cre recombinase, in one capsule. By presenting the VHH antibody with an affinity for cell-type-specific receptors such as the epidermal growth factor receptor (EGFR) on the capsule surface, we achieved cell-type selective endocytic uptake in A431 cell lines (high expression level of EGFR) over NHDF and MCF-7 cells (normal expression level of EGFR). This selective uptake was followed by the subsequent release of the encapsulated protein pharmaceuticals into the cytosol of the target cells. Unlike our previous version of the OLE-ZIP protein capsules modified with IgG antibodies, cytosolic delivery of pharmaceutical proteins was little impacted by the presence of other IgGs, which are abundant in the bloodstream. This improved characteristic suggests potential advantages for practical applications, including intravenous administration.

Introduction

The success of second-generation biopharmaceuticals based on antibodies has marked a significant shift from the traditional dominance of small organic molecule-based pharmaceuticals,[1] fuelling high expectations for the further advancement of biopharmaceuticals, including nucleic acid-based ones.[2] However, there are still concerns in the field of biopharmaceuticals arising from their inherent inability to spontaneously permeate cell membranes, attributed to the hydrophobic nature of these membranes.[3] This limitation results in low penetration efficiency, even at the single-cell level. Furthermore, in tissues where multiple cells are closely packed due to cell–cell adhesion (such as epithelial and muscle tissues) or cell–matrix adhesion (such as bone, nerve, and dermal tissues), the challenge of reduced permeability into the interior becomes more pronounced.[4] Another hurdle is the recognition of externally administered therapeutic proteins as 'foreign molecules' by the immune system, leading to their clearance through immune surveillance mechanisms.[5,6] A technology capable of enhancing membrane permeability not only at the single-cell level but also at the tissue level, while evading elimination mechanisms in the body, could not only enhance the therapeutic efficacy of conventional protein pharmaceuticals targeting cell membrane surfaces but also pave the way for a new generation of protein pharmaceuticals with the ability to target various biomolecules inside cells.

Traditionally, strategies to address these challenges have primarily focused on the development of techniques for membrane penetration at the single-cell level. This often involves conjugating proteins with amphiphilic and/or hydrophobic materials[7,8] that mimic the amphiphilicity of lipids constitut-

[a]Department of Life Science and Applied Chemistry, Graduate School of Engineering, Nagoya Institute of Technology, Gokiso-cho, Showa-ku, Nagoya, Aichi 466-8555, Japan. E-mail: toshitcm@nitech.ac.jp

[b]Graduate School of Pharmaceutical Sciences, Nagoya City University, 3-1 Tanabe-dori, Mizuho-ku, Nagoya 467-8603, Japan

[c]Faculty of Environmental Engineering, the University of Kitakyushu, 1-1 Hibikino, Wakamatsu, Kitakyushu, Fukuoka 808-0135, Japan

[d]Department of Biomolecular Engineering, Graduate School of Engineering, Tohoku University, Sendai, Miyagi 980-8579, Japan

[e]Department of Nanopharmaceutical Sciences, Graduate School of Engineering, Nagoya Institute of Technology, Gokiso-cho Showa-ku, Nagoya, Aichi 466-8555, Japan

†Electronic supplementary information (ESI) available. See DOI: https://doi.org/10.1039/d4pm00069b

ing cell membranes, thereby facilitating endocytic uptake. Cell Penetrating Peptides (CPPs)[9] are symbolic tools capable of conferring cell membrane permeability to exogenous proteins and peptides. Notable examples include TAT peptides,[10,11] Penetratin,[12] and Arginine-rich peptides.[13] It has been reported that by complexing these peptides with the exogenous proteins or peptides intended for delivery, in addition to endocytosis-mediated cell membrane permeability, energy-independent cell membrane permeability (translocation) may also be observed.

However, these approaches still face limitations in achieving efficient cytosolic delivery at the single-cell level. A more recent strategy involves manipulating the dynamics of membrane proteins between the inside and outside of cell membranes[14,15] or harnessing the channelling properties of channel membrane proteins.[16] To leverage these uptake routes, binding to target membrane proteins is essential. To confer targeting abilities, one reasonable strategy involves the conjugation of antibodies with high molecular discrimination capabilities. In this regard, VHH antibodies derived from camel antibody heavy chains[17] offer advantages. They have relatively low molecular weights (~15 kDa) compared to traditional IgG antibodies (150 kDa), making them easily conjugatable to pharmaceutical proteins through simple genetic modification. Moreover, it has been reported that surface modification of VHH *via* GPI-anchored membrane proteins can impart targeting capabilities to extracellular vesicles for drug delivery applications.[18]

Meanwhile, recently we reported a novel development in the form of protein capsules derived from the amphiphilic two-helix bundled protein OLE-ZIP, designed as a cell-permeable carrier for protein pharmaceuticals.[19,20] While the inherent OLE-ZIP protein capsule lacks cell membrane permeability, surface modification with IgG antibodies becomes a

key strategy. These antibodies exhibit affinity for cell-type-specific receptors present on the target cell surface, thereby facilitating cell-type selective cytosolic uptake of protein capsules *via* the receptor-mediated endocytic pathway.[21] The encapsulated protein pharmaceuticals are released into the cytosol, leveraging the pH-responsive property of OLE-ZIP to impart medicinal effects.[20] However, the practical application of OLE-ZIP protein capsules for intravenous administration[22] raised concerns due to the non-covalent immobilization of IgG antibodies on the capsule surface. To modify IgG on the capsule surfaces, we employed ProG-OLE-ZIP, a protein conjugate comprising the truncated Protein G (ProG) and OLE-ZIP components. The ProG domain allows for the reversible capturing of IgG onto the protein capsule surface at the constant region. Nevertheless, the high concentration of IgGs for other antigens (~11 g L^{-1}, ~80 μM) in the bloodstream[23] poses a potential risk of replacing and decreasing uptake efficiency and its cell-type selectivity.

In this study, we newly developed the intracellular delivery of protein pharmaceuticals using OLE-ZIP protein capsules, wherein VHH antibodies[17] were covalently linked to the OLE-ZIP protein capsule surfaces (Fig. 1). While cytosolic delivery can sometimes be defined as the transport of cargo such as proteins into the cytosol only through energy-independent mechanisms,[24] our previous study indicates that the protein transport using the OLE-ZIP protein capsules involves endocytosis-mediated cytosolic delivery,[25] as previously investigated.[20] Specifically, a VHH antibody with high affinity for the epidermal growth factor receptor (EGFR) was employed.[26] We evaluated the cytosolic delivery of encapsulated protein pharmaceuticals, such as RNase A[27,28] and Cre recombinase,[29,30] and its cell-type selectivity, focusing on EGFR-positive A431 cell lines.[31] Additionally, we investigated the potential impacts of contaminant IgGs on the cytosolic delivery of protein pharma-
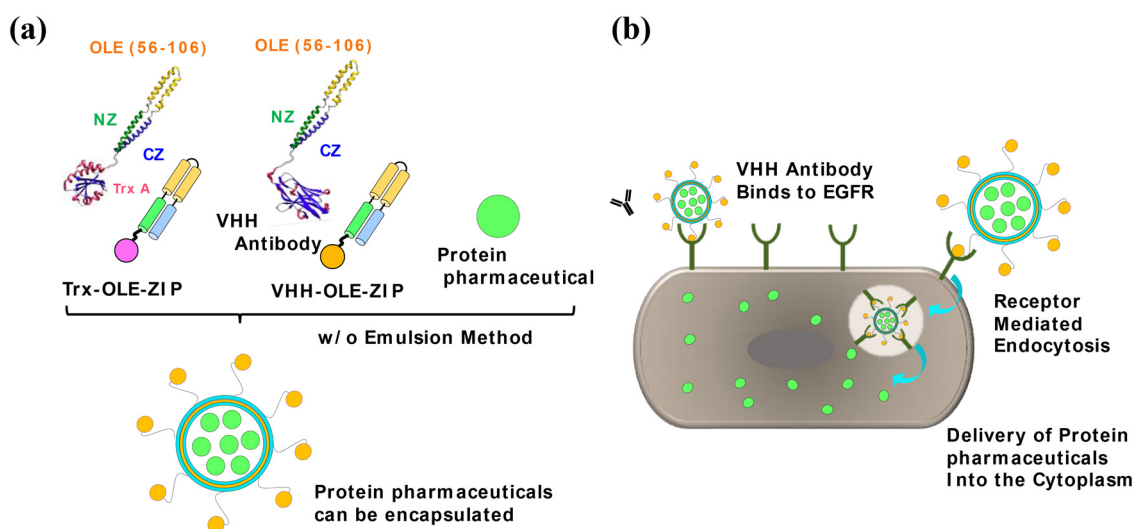

Fig. 1 Schematic illustration of cytosolic delivery of pharmaceutical proteins using the VHH-presented OLE-ZIP protein capsules. (a) Preparation of the VHH-presented OLE-ZIP protein capsules from Trx-OLE-ZIP and VHH-OLE-ZIP, encapsulating protein pharmaceuticals. (b) Proposed mechanism of cytosolic delivery of protein pharmaceuticals by the VHH-presented OLE-ZIP protein capsules *via* receptor-mediated endocytosis.

ceuticals using the VHH-presented OLE-ZIP protein capsules to A431 cell lines. Because of irreversible modification of antibodies to impart cell type selectivity, we anticipated cell-type selective delivery of protein pharmaceuticals, independent of the presence of IgG antibodies for other antigens abundantly present in the blood. This exploration aimed to pave the way for achieving cytosolic delivery of therapeutic proteins through intravenous administration.

Results and discussion

Preparation of capsule-forming amphiphilic proteins with VHH antibody moiety (VHH-OLE-ZIP-EV0, VHH-OLE-ZIP-EV1, and VHH-OLE-ZIP-EV2)

In the preparation of anti-EGFR VHH antibodies/OLE-ZIP conjugates, specifically denoted as VHH-OLE-ZIP, we constructed the *E. coli* expression vectors containing the requisite synthetic genes. For anti-EGFR VHH, we employed the mutant Ia1, reported by Roovers *et al.*[32] The OLE-ZIP component consists of the hydrophobic segment derived from the core hydrophobic region of sunflower oleosin (OLE(56–106)),[33–35] coupled with the hydrophilic segment derived from the heterodimeric coiled-coil peptides NZ and CZ.[36] The strategic linkage involved connecting NZ and CZ to the N- and C-terminal sides of OLE(56–108), respectively, facilitated by short linker peptides (GGSGGS). As demonstrated in our previous study,[20] OLE-ZIP adopts an overall two-helix-bundled structure. Its distinct amphiphilicity enables the formation of a protein-based bilayer structure resembling a phospholipid bilayer. Consequently, the utilization of a (w/o) emulsion method facilitates the generation of OLE-ZIP protein capsules, characterized by a capacious internal cavity.[19,20] The (w/o) emulsion method in this study includes these steps: first, in the presence of amphiphilic two helix-bundled proteins like OLE-ZIP, a small amount of buffer solution is ultrasonically dispersed into liquid paraffin, forming aqueous nano-droplets. The hydrophobic parts of OLE-ZIP cover the nano-droplets' surfaces facing the paraffin, while the hydrophilic parts face

inward, creating reverse micelles. This milky emulsion is placed on top of a fresh buffer solution, with remaining OLE-ZIP aligning at the emulsion-buffer interface. Centrifugation moves the OLE-ZIP-covered nano-droplets into the buffer, forming protein capsules with a bilayer membrane from the additional OLE-ZIP layer at the interface. While in this study, VHH-OLE-ZIP, wherein the anti-EGFR VHH is linked to the N-terminal side of OLE-ZIP through a linker peptide, newly served as the amphiphilic protein for capsule preparation. Through this molecular design, the surface of the resulting OLE-ZIP protein capsules was enveloped with VHH, thereby enabling cell-line selective uptake of the protein capsules. Nevertheless, concerns about the potential impact of the distance and flexibility of the VHH component from the capsule surface on cellular uptake efficiency prompted us to study additional conjugates. Consequently, we prepared expression vectors specific to the conjugates, incorporating one or two EV linkers[37] between the VHH and OLE-ZIP components (designated as VHH-OLE-ZIP-EV*n*, where *n* = 1 and 2, respectively). This strategic modification aimed to address and optimize the spatial dynamics, ensuring enhanced control over the efficiency of cellular uptake (Fig. 2(a)). EV linker is a non-natural linker peptide, including 26 SAGG repeats,[37] which has low propensity for specific secondary structure formation and is estimated to have a length of approximately 30 nm when fully extended. So, it should be suitable for a linker of VHH. In correspondence with this, the conjugate of OLE-ZIP and VHH lacking the EV linker were called, VHH-OLE-ZIP-EV0 as following.

The VHH-OLE-ZIP-EV*n* constructs (*n* = 0, 1, and 2) were initially produced in *E. coli* BL21(DE3) strains as fusion proteins with thioredoxin A. After cell lysis, purification of the fusion proteins from the supernatant fractions was achieved using Ni-affinity chromatography. Thrombin digestion was then employed to remove the thioredoxin A moiety, resulting in the final products VHH-OLE-ZIP-EV*n* (*n* = 0, 1, and 2) could be obtained. The amino acid sequences of VHH-OLE-ZIP-EV*n* (*n* = 0, 1, and 2) were summarized in Fig. S1.† Purity confirmation for each conjugate was performed through SDS-PAGE
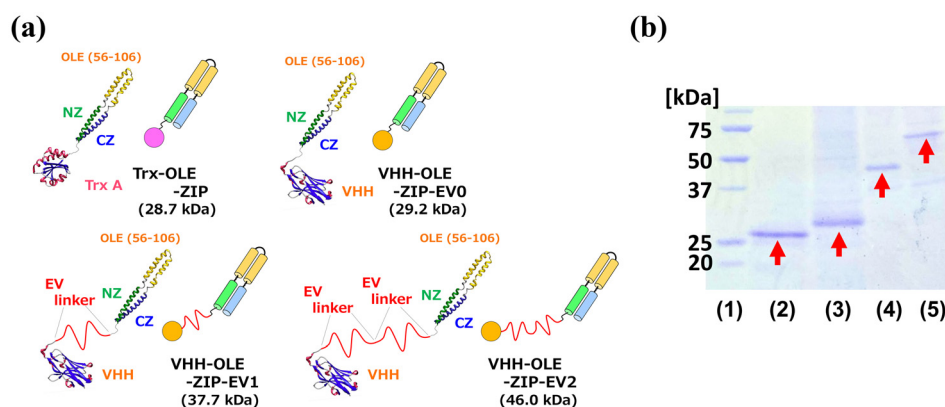

Fig. 2 (a) Schematic illustration of the OLE-ZIP mutants used in this study. (b) SDS-PAGE analyses of the OLE-ZIP mutants; MW marker (lane 1), Trx-OLE-ZIP (28.7 kDa, lane 2), VHH-OLE-ZIP-EV0 (29.2 kDa, lane 3), VHH-OLE-ZIP-EV1 (37.7 kDa, lane 4), and VHH-OLE-ZIP (46.0 kDa, lane 5).

analysis (Fig. 2(b)), and these proteins were subsequently employed in the ensuing experiments.

Protein capsule preparation and characterization

Similar to the challenges encountered in preparing protein capsules using ProG-OLE-ZIP,[19,20] the formation of capsules exclusively by VHH-OLE-ZIP-EVn (n = 0, 1, and 2) proved difficult, likely due to steric hindrance between the VHH components. Consequently, protein capsules were prepared utilizing a 9 : 1 mixture of Trx-OLE-ZIP and VHH-OLE-ZIP-EV0, VHH-OLE-ZIP-EV1, or VHH-OLE-ZIP-EV2 through a (w/o) emulsion method,[38] mirroring the approach used for ProG-OLE-ZIP. In subsequent experiments, protein capsules prepared from Trx-OLE-ZIP and VHH-OLE-ZIP-EV0, VHH-OLE-ZIP-EV1, or VHH-OLE-ZIP-EV2 were denoted as EV0, EV1, and EV2, respectively. Following capsule preparation, it was anticipated that EV0, EV1, and EV2 would present VHHs outward on the capsule surfaces *via* linker peptides (Fig. 3(a)).

The assessment of particle size and morphology of the prepared protein capsules, conducted through dynamic light scattering (DLS) and transmission electron microscopy,[39] is illustrated in Fig. 3(b) and (c). The results revealed the formation of a spherical morphology with an average diameter of approximately 70–200 nm. Notably, in terms of capsule formation, no significant impact of the difference in linker peptides of VHH-OLE-ZIP-EVn (n = 0, 1, and 2) was observed. Our

previous findings indicated that the loose molecular packing between the OLE-ZIP parts in the bilayer shells of Trx-OLE-ZIP protein capsules led to the lack of retention of staining dye within the inner aqueous phase during negative staining.[19,20] Consequently, the interior of EV0, EV1, and EV2 also exhibited whitening when stained with phosphotungstate salts in TEM measurements. While, TEM images at the outer edges of spherical capsules suggested the formation of bilayer shells comprising Trx-OLE-ZIP and VHH-OLE-ZIP-EVn (n = 0, 1, and 2).

To further confirm the bilayer structures, we conducted small-angle X-ray scattering (SAXS) measurements of EV0, EV1, and EV2 using the SPring-8 BL40B2 beamline. The flexibility of the VHH part in EV1 and EV2 possibly contributed to the inability to obtain clear X-ray scattering corresponding to shell parts. In contrast, EV0 exhibited sufficient X-ray scattering (Fig. 3(d)), aligning with a bilayer thickness of 5.5 nm, suggesting the formation of bilayer structures with two molecules of the OLE-ZIP parts in an apposed configuration. Similar X-ray diffractions and estimated shell thickness were observed for the protein capsules solely comprising Trx-OLE-ZIP or a 9 : 1 mixture of Trx-OLE-ZIP and ProG-OLE-ZIP.[20] These results further supported the successful preparation of a bilayer shell comprising Trx-OLE-ZIP and VHH-OLE-ZIP-EV0 in EV0.

To assess the thermal stability of the capsules, we conducted measurements of the temperature-dependent alteration
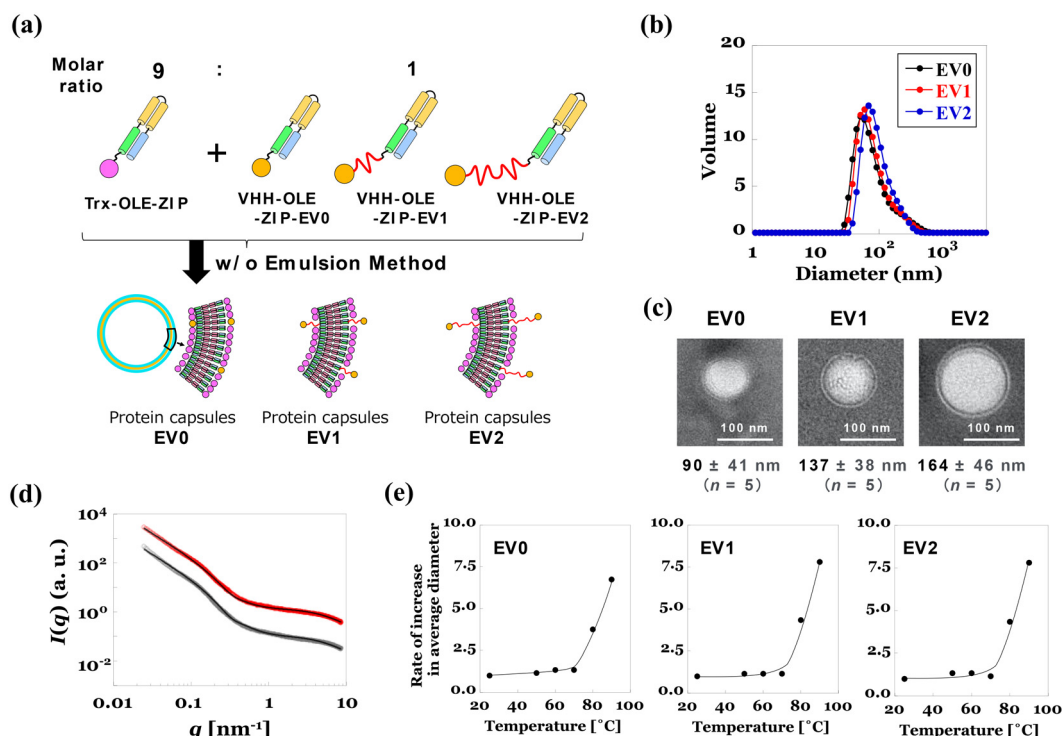

Fig. 3 (a) Preparation of the protein capsules of Trx-OLE-ZIP and VHH-OLE-ZIP-EVn (n = 0, 1, and 2) in the molar ratio of 9 : 1. (b) DLS profiles of the protein capsules prepared from Trx-OLE-ZIP and VHH-OLE-ZIP-EVn (n = 0, 1, and 2). (c) TEM measurements of the protein capsules prepared from Trx-OLE-ZIP and VHH-OLE-ZIP-EVn (n = 0, 1, and 2). (d) SAXS analysis of the protein capsules EV0 with or without encapsulating the cargo protein, GFP, in 50 mM Tris HCl buffer (pH 7). (e) Impact of short heat treatment (20–100 °C) for 15 min on average diameters of the protein capsules, prepared from Trx-OLE-ZIP and VHH-OLE-ZIP-EV0, VHH-OLE-ZIP-EV1, or VHH-OLE-ZIP-EV2.

of the dynamic light scattering (DLS) peak. The results, presented in Fig. 3(e), demonstrated that, similar to protein capsules consisting solely of Trx-OLE-ZIP,[19] all the capsules maintained a homogeneous dispersion as single particles in an aqueous buffer up to 50 °C. However, beyond this temperature range, a gradual increase in particle size with the rise in temperature was observed. This increase suggested the formation of aggregates, potentially induced by destabilization in the protein folding of the OLE-ZIP components.

Next, to assess the encapsulation abilities of EV0, EV1, and EV2 for guest proteins, we introduced FITC-labelled RNaseA and conducted gel permeation chromatography (GPC) analysis. The GPC chromatograms obtained (Fig. S2†) revealed that the GPC peak corresponding to RNaseA-encapsulated protein capsules shifted relative to that of free RNaseA. This shift indicated that EV0, EV1, and EV2 could effectively retain guest proteins within the inner aqueous phase while maintaining the capsule morphologies even under infinite dilution conditions. Subsequent SDS-PAGE analyses of the isolated peak of the RNaseA-encapsulated protein capsules demonstrated the simultaneous presence of RNaseA, Trx-OLE-ZIP, and VHH-OLE-ZIP-EVn (n = 0, 1, and 2) (Fig. S3†). This observation suggested the stable encapsulation of guest proteins within the inner aqueous phase of EV0, EV1, and EV2. Considering the average capsule diameters, molecular size of the OLE-ZIP part, and the number of encapsulated RNaseA molecules, we estimated that each capsule can hold approximately ~400 molecules of RNaseA. In TEM measurements (Fig. S4†), unlike the empty protein capsules, a distinct dark contrast was evident within the capsule interior, supporting the idea that the interior of the capsules was filled with guest proteins. Furthermore, SAXS measurements revealed X-ray diffractions originating from the encapsulated guest proteins, a phenomenon distinct from the empty protein capsules (Fig. 3(d)). These findings collectively support the notion that the capsule interior is densely filled with the cargo protein.

Evaluation of cellular uptake behaviours and its cell-type selectivity of the OLE-ZIP protein capsules

To assess the ability of protein capsules EV0, EV1, and EV2 for the cytosolic delivery of cargo proteins, we initially investigated the uptake efficiency and cell-line selectivity of the empty protein capsules using confocal laser scanning microscopy (CLSM) and fluorescence-activated cell sorting (FACS) measurements. To track their uptake processes through fluorescence, the FITC-labelled Trx-OLE-ZIP was used for capsule preparation. Fig. 4(a) presents CLSM images of A431 cells after incubating the FITC-labelled EV0, EV1, and EV2 (total concentration of capsule-forming proteins set at 1 μM) in DMEM with 10% FBS for 12, 24, 48, and 72 h at 37 °C. A431 cells were chosen as a representative mammalian cell line expressing a high level of EGFR.[31] So, uptake via receptor (in this case, EGFR)-mediated endocytosis was anticipated. Since the VHH antibody used here is not the natural ligand for EGFR, we think that protein capsules are internalized into the cells through receptor-binding-mediated endocytosis, which is different from the typical receptor-dependent endocytosis activated by ligand binding.[40] Therefore, like our previous evaluation of the cellular uptake of OLE-ZIP protein capsules modified with IgG antibodies,[20] we predict that a culture time of more than 12 hours is required for sufficient cellular uptake. Despite the protein capsules adsorbing onto cell surfaces without internalization, which persisted even after PBS washes, a discernible preference for uptake by A431 cells was observed from CLSM observations (Fig. 4(a)). To quantify uptake efficiencies precisely, remaining capsules on cell surfaces were removed by trypsin digestion, and FACS analyses were conducted. Fig. 4(b) indicated the gradual increase in FITC fluorescence from cells with an extended incubation time, indicating a time-dependent uptake. Notably, when normalized to 1 for EV0 after 24 hours of incubation, the order of uptake efficiencies was EV2 > EV1 > EV0. When the uptake efficiency was normalized to 1 for EV0 after 24 h of incubation, it increased to 1.1 for EV1 and 1.3 for EV2. Even after 72 h of incubation, these ratios were almost sustained (1.1 for EV1 and 1.7 for EV2). It suggested that longer linker peptides were associated with higher uptake efficiency.

While, NHDF cells were chosen as a negative control for the uptake experiments, as they express a normal level of EGFR, thus anticipating lower uptake efficiency compared to A431 cells. Fig. 4(c) indeed shows less uptake to NHDF cells after 24 and 48 h of incubation. FACS analyses in Fig. 4(d) provide a quantitative evaluation of the selectivity for A431 over NHDF after 24 h of EV0 incubation, estimating a 7.1-fold selectivity. This result implies that the VHH-presenting protein capsule demonstrates cell-type selective uptake guided by the interactions between VHH and EGFR. The observed selectivity supports the potential of these protein capsules for targeted cytosolic delivery to specific cell types expressing the target receptor.

Next, to evaluate delivery efficiency of cargo proteins, we first did experiments using RNase A as a cargo protein. Pancreas RNase A is known to induce cytotoxicity, which if observed would indicate successful uptake into the cytoplasm of cancerous cell line such as A431.[27,28] So, from IC$_{50}$ (μM) ability of cytosolic delivery could be estimated. Preparations of the RNase A-loaded protein capsules, EV0, EV1, and EV2 were performed as similarly to that without encapsulating cargo proteins. From DLS and TEM measurements, spherical morphologies with similar average diameters were retained as similar to the originals. The average loading amount of RNase A versus total concentration of capsule forming OLE-ZIP proteins in protein capsule was 0.95 μM of RNaseA: 10 μM of capsule forming OLE-ZIP proteins.

To clarify the target-selective cytotoxicity, we first examined cell viability in A431 cells upon adding RNase A-loaded EV0. The obtained data is summarized in Fig. 4(e), showing a clear decrease in cell viability. When adding free RNase A (10 μM), empty EV0, or Trx-OLE-ZIP protein capsules encapsulating RNase A (0.95 μM), no decrease in cell viability was observed. This indicates that VHH-guided delivery of encapsulated RNase A can be effectively performed using EV0. Additionally,
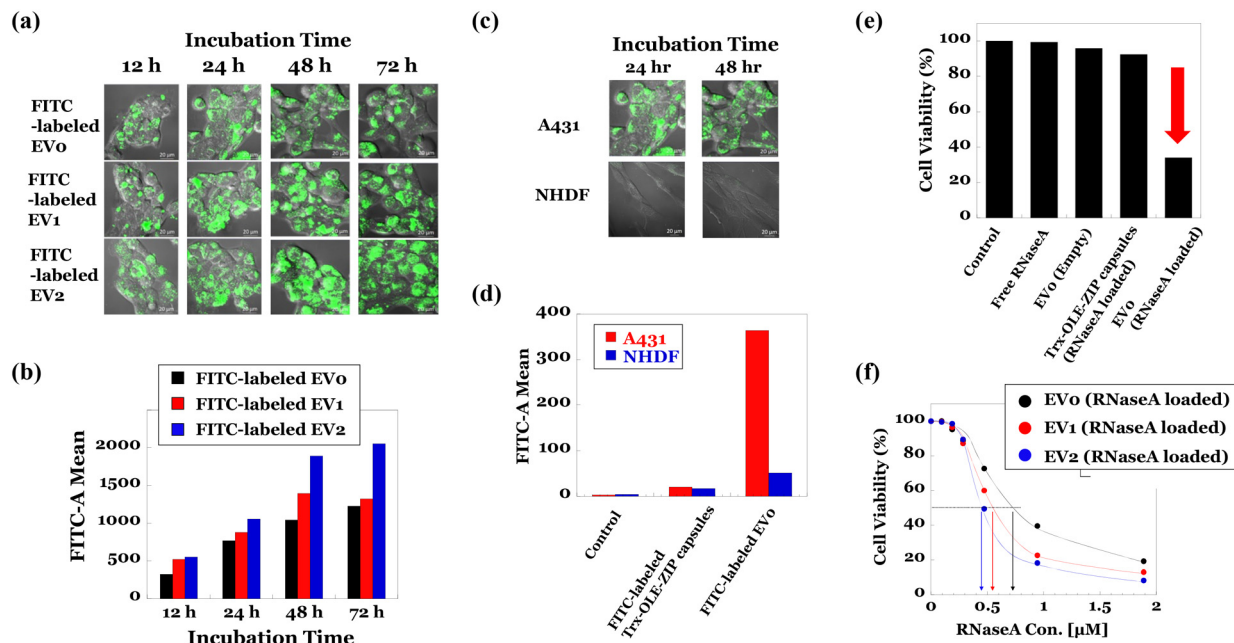
Fig. 4 (a) CLSM observation of the A431 cells after incubation of the FITC-labelled EV0, EV1, and EV2 (the total concentrations of capsule forming proteins were set by 1 μM) for 12, 24, 48 and 72 h at 37 °C. (b) FACS analyses of the A431 cells after incubation of the FITC-labelled EV0, EV1, and EV2 (the total concentrations of capsule forming OLE-ZIP proteins were set by 1 μM) 12, 24, 48 and 72 h at 37 °C. To harvest A431 cells from culture dish for FACS observation, trypsin digestion was applied. (c) CLSM observation of the A431 cells or NHDF cells after incubation of the FITC-labelled EV0 (the total concentration of capsule forming OLE-ZIP proteins was set by 1 μM) for 24 and 48 h in DMEM with 10% FBS at 37 °C. (d) FACS analyses of the A431 cells or NHDF cells after incubation of the FITC-labelled Trx-OLE-ZIP capsules or the FITC-labelled EV0 (the total concentration of capsule forming OLE-ZIP proteins was set by 1 μM) for 24 h in DMEM with 10% FBS at 37 °C. For the control samples, A431 and NHDF cells cultured for 24 hours without any additions were used. To harvest both cells from culture dish for FACS observation, trypsin digestion was applied. (e) Comparison of A431 cells' viabilities (%) after 72 h incubation of free RNase A (10 μM), EV0 (Empty) (No RNaseA was loaded and the total concentration of capsule forming proteins was set by 10 μM), Trx-OLE-ZIP protein capsules (RNaseA loaded) (0.95 μM of RNaseA was loaded and the concentration of Trx-OLE-ZIP was set by 10 μM), and EV0 (RNaseA loaded) (0.95 μM of RNaseA was loaded and the total concentration of capsule forming protein was set by 10 μM) at 37 °C. (f) Concentration dependence of the RNaseA-loaded EV0, EV1, and EV2 (the concentration of RNaseA was varied from 0–1.9 μM) on A431 cells' viability (%) after 72 h incubation at 37 °C.

to assess the impact of linker length on cytotoxicity, we measured cell viability after incubating with different concentrations of RNase A-loaded protein capsules (EV0, EV1, and EV2) for 72 hours (Fig. 4(f)). The estimated IC_{50} values (μM) were 0.45, 0.53, and 0.72, respectively, indicating that increasing linker length slightly improved the IC50 as anticipated.

Using EV2 as the most effective carrier for cytosolic delivery from the above experiments, we extended our investigations to use Cre recombinase as a cargo protein. Cre recombinase is an enzyme that catalyses homologous recombination of DNA flanked by LoxP sequences.[29] In the case of successful uptake of Cre recombinase to the target cells harbouring the Cre spotlight DNA sequence[41] in their chromosomal DNA, the DsRed expression can be switched to the GFP by eliminating the DsRed gene part, flanked between the LoxP sequences, in their chromosomal DNAs (Fig. 5(a)). To elucidate the efficiency in cell-type selective delivery, we constructed the gene-modified A431 (EGFR-positive) and MCF-7 (EGFR-normal) cell lines, both of which have chromosomal DNAs containing the Cre Spotlight DNA sequence.

As shown in the CLSM observations of A431 and MCF-7 cells (Fig. 5(b)), after incubation of the Cre recombinase-loaded EV2 (total concentration of capsule forming proteins were set by 1 μM. Cre recombinase concentration was 0.095 μM) for 72 h colour change of A431 cells from red to orange was successfully observed only the case when A431 cells were incubated with the VHH-presented Cre-recombinase-encapsulated EV2. Because more than 24 h incubation is necessary for efficient delivery of RNase A to cytosol, total fluorescence colour of the resulting cells became a mixture of DsRed (previously expressed) and GFP (newly expressed after Cre recombinase delivery). For MCF-7 cells, a slight increase in GFP-derived fluorescence intensity was observed even when only Cre recombinase was added, suggesting that Cre recombinase itself is slightly taken up by MCF-7 cells. However, when Cre recombinase was encapsulated in EV2 and added, no greater increase in GFP-derived fluorescence intensity was observed compared to when Cre recombinase was added alone, suggesting that encapsulation in EV2 did not enhance the uptake of Cre recombinase. These data indicated that cell line-selective cytosolic delivery could be achieved as anticipated. The FACS analysis of the same samples also supported that the above fluorescence colour change was performed only of A431 cells (Fig. 5(c)).
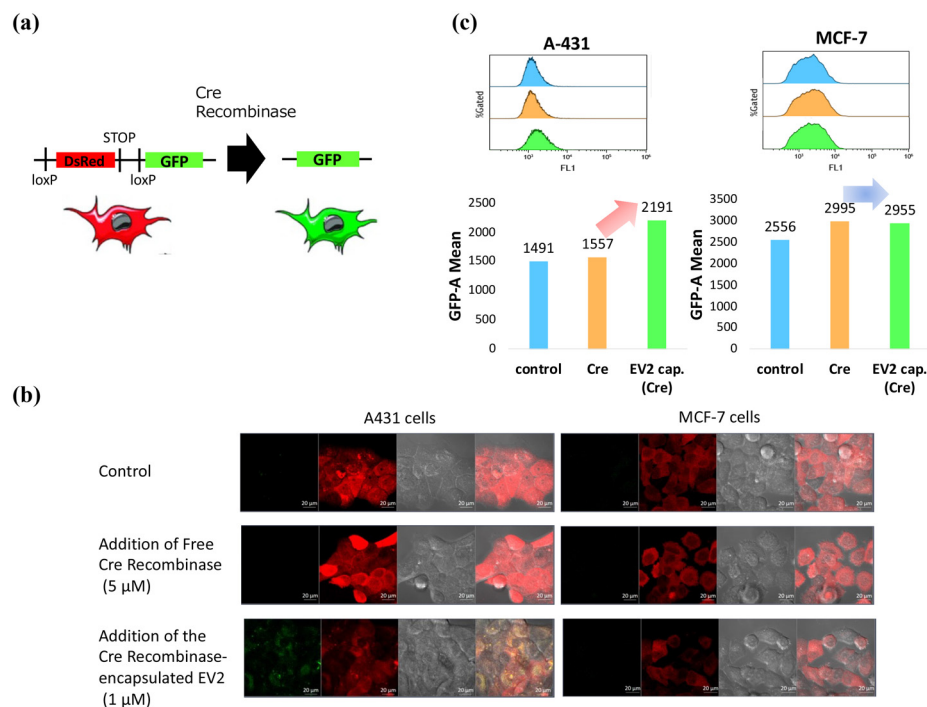
Fig. 5 Cytosolic delivery of Cre recombinase using the VHH-presented EV2 (the total concentration of capsule forming OLE-ZIP proteins was set by 1 μM, Cre recombinase 0.095 μM) for A431 and MCF-7 cells. Both cells constantly express DsRed from the Cre spotlight gene. (a) Set-up of Cre spotlight gene, consisting of the DsRed gene, flanked between loxP. (b) CLSM observation of A431 and MCF-7 cells after incubation of the Cre-recombinase-encapsulated EV2 for 72 h at 37 °C. (c) FACS analyses of GFP fluorescence from A431 and MCF-7 cells after incubation of the Cre-recombinase-encapsulated EV2 for 72 h at 37 °C.

Comparison of the impacts of the contaminant of other IgG on cytosolic delivery by OLE-ZIP protein capsules

Unlike the case of presenting IgG, the VHH-presented protein capsules were anticipated to exhibit cell-type selective uptake irrespective of contaminant IgGs, which were expected when the protein capsules were administered into the bloodstream,[23] containing abundant other IgGs for different antigens. To verify this advantage, we used RNase A as a cargo protein (0.47 μM) in this experiment and compared cell viability in the presence of other IgG between using IgG-presented protein capsules and using VHH-presented EV2 (total concentrations of capsule-forming proteins were set by 5 μM). Anti-CD20 IgG, orizumab, was chosen as a representative contaminant, as it has no impact on the cell viability of A431 cell lines.[42]

As shown in Fig. 6, when the RNase A-containing protein capsules presenting Cetuximab were added to A431 cells, a significant reduction in cytotoxicity was observed upon co-addition of the competing IgG antibody, Omalizumab (cell viability (%) increased from 67% to 80%) with comparison to no addition of Omalizumab. On the other hand, when the RNase A-containing EV2 presenting VHH antibodies were added, there was little reduction in cytotoxicity upon co-addition of Omalizumab (cell viability (%) increased only slightly from 41% to 44%). These results suggest that, as initially feared, in the presence of competing IgG antibodies, the initially-presented IgG antibodies to induce receptor-mediated endocytosis
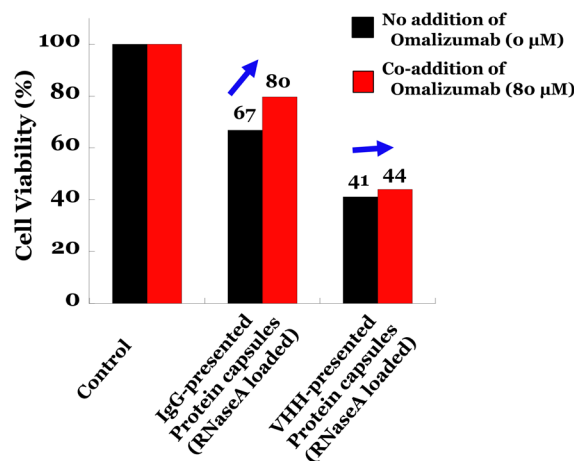

Fig. 6 Comparison of the impacts on cell viability of A431 cells upon delivering RNase A by the IgG(cetuximab)-presented protein capsules or the VHH-presented protein capsules (EV2) (in both cases, the total concentrations of capsule-forming proteins were set by 5 μM, the concentrations of RNase A was 0.47 μM, the concentration of cetuximab was 0.5 μM), in the presence (80 μM) or absence of competitive IgG antibody, Omalizumab, after 72 h incubation at 37 °C.

(in this case, cetuximab) are replaced by the co-existing IgG antibodies, leading to a significant decrease in cellular uptake. This also implies that the additional role of the presented IgG antibodies in providing cell-type selectivity is also compro-

mised when replaced by other IgG antibodies. Particularly in the bloodstream, where concentrations of IgG antibodies reach around 80 μM,[23] practical use through intravenous administration of the IgG-presented protein capsules is suggested to be challenging. On the other hand, the RNase A-containing EV2 presenting VHH antibodies did not show a significant reduction in cytotoxicity in the presence of competing IgG antibodies. Therefore, these data suggests that for the practical usability of OLE-ZIP protein capsules through intravenous administration, the VHH-presented OLE-ZIP protein capsule is a promising candidate for new cytosolic carrier of various pharmaceutical proteins.

Conclusions

In this study, we explored the development of a novel protein delivery technology based on protein capsules formed by an amphiphilic two-helix-bundled protein OLE-ZIP, allowing cell-type selectivity through the presentation of VHH antibodies. We designed VHH-OLE-ZIP by introducing the C-terminal side of VHH antibodies with affinity to EGFR to the N-terminal of OLE-ZIP *via* a flexible linker peptide. The OLE-ZIP part was previously proven to have capsule-forming ability. Successfully constructing OLE-ZIP protein capsules with an average diameter of around 100 nm, where VHH is tethered to the capsule surface, was achieved by mixing it with Trx-OLE-ZIP in a 1 : 9 ratio. For capsule formation, we employed an (w/o) emulsion method, dissolving the protein of interest in the aqueous buffer for precursor solution of inner aqueous phase, enabling the encapsulation of various water-soluble proteins such as GFP, RNase A, and Cre Recombinase. The capsules, with sufficient internal space, allowed the encapsulation of around 400 molecules of each protein per capsule. Furthermore, these protein capsules maintained stably dispersed in a buffer up to approximately 50 °C, with their individual particle integrity.

Additionally, VHH antibody presentation facilitated preferential uptake to A431 cell lines expressing high levels of EGFR, exhibiting a selectivity approximately 7.1-times greater than that to the fibroblast cell line, NHDF. Regarding the binding affinity of VHH antibodies presented on the capsule surface to EGFR on the target cell membrane, we anticipated a dependency on the orientational freedom of the VHH segment. To clarify this impact, we constructed the VHH-OLE-ZIP variants, VHH-OLE-ZIP-EVn (n = 0, 1, and 2), with varied linker length between the VHH and OLE-ZIP segments. By using these variants to prepare the protein capsules (EV0, EV1, and EV2), we compared cellular uptake efficiency and cell-type selectivity. Notably, EV2, with the longest linker length, demonstrated a certain superiority in these aspects.

Finally, we simulated an environment with concomitance of other IgGs like the bloodstream upon concomitance of anti-CD20 IgG (10 μM) in DMEM and evaluated the impact on the uptake efficiency of RNase A to A431 cells using the IgG-presented OLE-ZIP capsules and VHH-presented OLE-ZIP capsules. The results showed a significant reduction in uptake efficiency for OLE-ZIP protein capsules when presenting IgG antibodies cetuximab, on the surface. On the other hand, with the OLE-ZIP protein capsules presenting VHH antibodies, the influence of adding anti-CD20 IgG antibodies (10 μM) was minimal, demonstrating the effectiveness of these capsules as promising carriers for intracellular delivery of therapeutic proteins *via* intravenous administration.

To achieve more efficient cytosolic delivery of pharmaceutical proteins in a shorter time by OLE-ZIP protein capsules, optimization of the VHH antibodies for suitable target membrane proteins onto target cell membranes is deemed necessary. Additionally, optimizing the capsule-forming protein segment to enable efficient release from endosomes would also be crucial. These considerations continue to be the focus of ongoing research in our laboratory.

Experimental

Materials

Restriction enzymes, alkaline phosphatase, and Normal Human Dermal Fibroblasts (NHDF) cell were purchased from Takara-bio. Inc. (Japan). Taq DNA polymerase (AmpliTaq Gold DNA polymerase) was purchased from Thermo Fisher Scientific K.K. (Japan). Rapid DNA Ligation Kit, pET-32a (+) DNA, and fluorescein isothiocyanate (FITC) was purchased from Merck KGaA (Germany). Tris(hydroxymethyl)aminomethane (Tris), isopropyl-β-D-thiogalactopyranoside (IPTG), agar, Agarose ME, Ampicillin Sodium, lysogeny broth medium (Lennox), DMEM, penicillin–streptomycin (100 U mL^{-1}), and CCK-8 were purchased from Wako Chemicals (Japan). Sephadex G-50 was purchased from Cytiva (Japan). Oligo DNAs for genetic mutations by PCR was purchased from Eurofins Genomics Co Ltd (Japan). Ribonuclease A from Bovine Pancreas was purchased from Nacalai Tesque Inc. (Japan). A431 cell (JCRB0004) was supplied from JCRB cell bank (Japan). Trx-OLE-ZIP was prepared as following the previous study.[20] Cre recombinase was produced by *E. coli* BL21(DE3) expression system using the expression vector, supplied from Addgene (Plasmid# 62730). To construct the A431 and MCF-7 cell lines, stably expressing Cre spotlight gene, were prepared by transfection of the nicked plasmid of Cre spotlight (Addgene, Plasmid# 45150). Other chemicals were used without further purification.

Expression of VHH-OLE-ZIP-EVn (n = 0, 1, and 2)

A DNA fragment with NcoI and HindIII restriction enzyme sites at each end, encoded for VHH-OLE-ZIP-EVn (n = 0, 1, or 2) was inserted into a modified pET-32a(+) plasmid vector, which lacked the genes for S-tag and the enterokinase digestion site from the original. The expressed protein became a fusion protein, composed of thioredoxin A (Trx) and VHH-OLE-ZIP-EVn (n = 0, 1, or 2). *Escherichia coli* BL21(DE3) cells were transformed with the plasmid, and were cultured in LB medium (Lennox) supplemented with ampicillin (100 μg mL^{-1}) at 37 °C for 3 h, and for an additional 3 h at 37 °C in

the presence of 1 mM IPTG. The cells were harvested, resuspended in 50 mM Tris HCl buffer (pH 7) with 100 mM NaCl and 10 (v/v)% glycerol, and sonicated. The supernatant fraction was subjected to Ni-NTA affinity chromatography to isolate the target fusion protein. Then the purified fusion protein (~10 mg) was further digested by thrombin (0.1 mg) in 20 mL of thrombin buffer (20 mM Tris HCl (pH 8.4), 150 mM NaCl, 20 mM CaCl$_2$) at 4 °C overnight and VHH-OLE-ZIP-EVn (n = 0, 1, or 2) was isolated by Ni-NTA affinity chromatography again. The purity of target protein was analysed by SDS-PAGE analysis.

FITC-labelling of Trx-OLE-ZIP

Referring the previous study,[43] we prepared the FITC-labelled OLE-ZIP. Briefly, 20 mg (0.73 μmol) of Trx-OLE-ZIP was suspended in 10 mL of 50 mM carbonate buffer (pH 10) and kept at 4 °C for 30 min. FITC (0.57 mg, 1.46 μmol) was then added to the suspension, which was shaken overnight at 150 rpm using an orbital shaker (CD-100e, EYELATEC, Japan). The FITC-labelled Trx-OLE-ZIP was obtained as an insoluble fraction after solvent exchange to deionized water. The FITC-labelled Trx-OLE-ZIP was purified by washing it thrice in deionized water. Any unreacted FITC was removed and checked by SDS-PAGE before use.

Preparation of the protein capsules of Trx-OLE-ZIP and VHH-OLE-ZIP-EVn (n = 0, 1, and 2), EV0, EV1, and EV2

For preparation of protein capsules of the 9 : 1 mixture of Trx-OLE-ZIP and VHH-OLE-ZIP-EV0, VHH-OLE-ZIP-EV1, or VHH-OLE-ZIP-EV2, 25 μL of inner aqueous phase solution (50 mM phosphate buffer (pH 7), 150 mM sucrose) and 25 μL of TFE solution of the 9 : 1 mixture of Trx-OLE-ZIP and VHH-OLE-ZIP-EVn (n = 0, 1, or 2) (total concentration of proteins was 200 μM) were added to 500 μL of liquid paraffin and it was sonicated to be a homogeneous emulsion by using an ultrasonic disruptor (UD-211, TOMY SEIKO Co. Ltd, Japan). The obtained emulsion was piled onto 500 μL of 50 mM phosphate buffer (pH 7) in 1.5 mL tube and this two-phase solution was applied centrifugation (12 000g) for 15 min at ambient temperature.

DLS analyses of the protein capsules EV0, EV1, and EV2

The mean hydrodynamic diameter of protein capsules of Trx-OLE-ZIP and ProG-OLE-ZIP was estimated using a Zetasizer Nano ZS (Malvern Instruments Ltd).

TEM measurements of spherical morphologies of protein capsules EV0, EV1, and EV2

TEM images were obtained with JEM-z2500 (JEOL). All samples were supported by dry-cast of protein solutions on a poval-coated Cu grid. The protein capsule solution was dropped Cu grid, after stand for approximately 5 min at room temperature. Droplets were removed with filter paper and stain by sodium phosphotungstate.

SAXS analysis of the protein capsules EV0

X-ray scattering measurements were performed at the SPring-8 BL40B2 beamline. A 25.4 × 28.9 cm^2 photon-counting detector (PILATUS3 S 2M, Dectris, Switzerland) was placed 1.0 or 4.0 m from the sample. The wavelength (λ) of the incident X-rays was 1.0 Å. The OLE-ZIP protein capsule solution in Tris HCl (pH 7) was packed into a quartz capillary cell with a light path length of 2 mm. The incident X-ray wavelength, λ, was fixed at 0.71 c5. The correct path length was determined using silver behenate and the magnitude of the scattering vector [$q = (4\pi/\lambda) \sin \theta/2$] with the scattering angle of θ. The scattering intensities as 2D spectra were transformed into 1D profiles by circular averaging to obtain the data set of the scattering intensity [$I(q)$ and q].

Evaluation of uptake behaviours of the FITC-labelled protein capsules EV0, EV1, and EV2 to A431 or NHDF cell lines using confocal laser scanning microscope (CLSM)

A431 or NHDF cells (1 × 10^5 cells per well) were seeded onto a glass-base dish (AGC Techno Glass Co. Ltd, Japan) and incubated in DMEM supplemented with 100 U mL^{-1} penicillin–streptomycin solution and 10% FBS overnight under 5% CO$_2$ at 37 °C. After removing the medium, 1 μM solution of the protein capsule (EV0, EV1, or EV2) was added to cells for 12, 24, 48 or 72 h at 37 °C. The FITC-labelled Trx-OLE-ZIP was used for this experiment. After removal of the protein capsules solution, the cells were washed in PBS thrice, re-suspended in DMEM without phenol red, and then subjected to CLSM observation.

Evaluation of uptake behaviours of the FITC-labelled protein capsules (EV0, EV1, and EV2) to A431 or NHDF cell lines using fluorescence activated cell sorting (FACS) analysis

A431 or NHDF cells (5 × 10^5 cells per well) were seeded onto a 6-well plate and incubated in DMEM supplemented with 100 U mL^{-1} penicillin–streptomycin solution and 10% FBS overnight under 5% CO$_2$ at 37 °C. After removing the medium, 1 μM solution of the protein capsule (EV0, EV1, or EV2) was added to cells for 12, 24, 48 or 72 h at 37 °C. The FITC-labelled Trx-OLE-ZIP was used for this experiment. After removal of the protein capsule solution, the cells were washed in PBS thrice. After detachment of cells using 0.25 w/v% trypsin-1 mmol L^{-1} EDTA·4Na solution, the cells were collected by centrifuge and washed in PBS thrice. The collected cells were resuspended in PBS with 3% FBS and it was subjected to FACS analyses using FACSVerse (BD Biosciences, USA).

Preparation of the protein capsules (EV0, EV1, and EV2), encapsulating GFP, RNaseA, or Cre recombinase

For preparation of the protein capsules EV0, EV1 and EV2, encapsulating GFP, RNaseA, or Cre recombinase, 25 μL of the inner aqueous phase solution (50 mM phosphate buffer (pH 7), 150 mM sucrose) with 40 μM of GFP, RNaseA, or Cre recombinase was used instead of that without RNase A. Preparation

process was similar to that without RNase A. For isolation of the protein capsules with GFP, RNaseA, or Cre recombinase, gel permeation chromatography (1 cm (i.d.) × 50 cm (h), Sephadex G-50) was applied using 50 mM phosphate buffer (pH 7) as an elution buffer.

Evaluation of cytosolic delivery of RNase A, by encapsulating in the protein capsules (EV0, EV1, and EV2) from induction of cytotoxicity, IC_{50} (μM)

A431 cells (1×10^4 cells per well) were seeded onto a 96-well plate and incubated in DMEM supplemented with 100 U mL^{-1} penicillin–streptomycin solution and 10% FBS overnight under 5% CO_2 at 37 °C. After removing the medium, the RNase A-encapsulated protein capsules (EV0, EV1, or EV2) (1 μM), were added to the cells for 72 h at 37 °C. After removal of the protein cage solution, the cells were washed in PBS thrice and subjected to CCK-8 assay to estimate the number of live cells. Using a non-linear-curve-fitting analysis, the IC50s (μM) were estimated as an index of uptake efficiency.

Evaluation of cytosolic delivery of Cre recombinase by encapsulating in the protein capsules, EV2, by CLSM

A431 or MCF-7 cells (1×10^5 cells per well), which constantly express the translational product from the Cre spotlight gene,[41] were seeded onto a glass-base dish (AGC Techno Glass Co. Ltd, Japan) and incubated in DMEM supplemented with 100 U mL^{-1} penicillin–streptomycin solution and 10% FBS overnight under 5% CO_2 at 37 °C. After removing the medium, 1 μM solution of the protein capsule (EV0, EV1, or EV2), encapsulating Cre recombinase (0.095 μM) was added to cells for 72 h at 37 °C. After removal of the protein capsules solution, the cells were washed in PBS thrice, re-suspended in DMEM without phenol red, and then subjected to CLSM observation.

Evaluation of cytosolic delivery of Cre recombinase by encapsulating in the protein capsules, EV2, by FACS

A431 or MCF-7 cells (5×10^5 cells per well), which constantly express the translational product from the Cre spotlight gene, were seeded onto a 6-well plate and incubated in DMEM supplemented with 100 U mL^{-1} penicillin–streptomycin solution and 10% FBS overnight under 5% CO_2 at 37 °C. After removing the medium, 1 μM solution of the protein capsule (EV0, EV1, or EV2), encapsulating Cre recombinase (0.095 μM) was added to cells for 72 h at 37 °C. After removal of the protein capsule solution, the cells were washed in PBS thrice. After detachment of cells using 0.25 w/v% trypsin-1 mmol L^{-1} EDTA·4Na solution, the cells were collected by centrifuge and washed in PBS thrice. The collected cells were resuspended in PBS with 3% FBS and it was subjected to FACS analyses using GALLIOS (Beckman Coulter, Inc., USA).

Comparison of cytotoxicities when incubating RNaseA-loaded EV2 *versus* RNaseA-loaded Trx-OLE-ZIP/ProG-OLE-ZIP protein capsules with the supplementation of cetuximab, in the presence or absence of the competitive IgG antibody, Omalizumab

A431 cells (1×10^4 cells per well) were seeded onto a 96-well plate and incubated in DMEM supplemented with 100 U mL^{-1} penicillin–streptomycin solution and 10% FBS overnight under 5% CO_2 at 37 °C. After removing the medium, the RNase A-encapsulated EV2 (5 μM) or the RNaseA-loaded Trx-OLE-ZIP/ProG-OLE-ZIP protein capsules (5 μM) with supplement of cetuximab (0.5 μM), were added to the cells for 72 h at 37 °C. To clarify the impacts of existence of competitive IgG, Omalizumab, we did the same experiments in the presence of 80 μM of Omalizumab. After removal of the protein capsule solution, the cells were washed in PBS thrice and subjected to CCK-8 assay to estimate the number of live cells.

Author contributions

Data availability

The raw data supporting the findings of this study will be uploaded to your website, but if you wish to provide it to a third party, please request prior permission from the corresponding author, T.M.

Conflicts of interest

There are no conflicts to declare.

Acknowledgements

References

1 M. Kesik-Brodacka, *Biotechnol. Appl. Biochem.*, 2018, **65**, 306–322.

2 A. Khvorova and J. K. Watts, *Nat. Biotechnol.*, 2017, **35**, 238–248.

3 M. P. Stewart, R. Langer and K. F. Jensen, *Chem. Rev.*, 2018, **118**, 7409–7531.

4 P. Chames, M. Van Regenmortel, E. Weiss and D. Baty, *Br. J. Pharmacol.*, 2009, **157**, 220–233.

5 I. R. Correia, *mAbs*, 2010, **2**, 221–232.

6 R. Dingman and S. V. Balu-Iyer, *J. Pharm. Sci.*, 2019, **108**, 1637–1654.

7 Y. W. Lee, D. C. Luther, R. Goswami, T. Jeon, V. Clark, J. Elia, S. Gopalakrishnan and V. M. Rotello, *J. Am. Chem. Soc.*, 2020, **142**, 4349–4355.

8 Y. H. Wu, L. Jiang, Z. X. Dong, S. X. Chen, X. Y. Yu and S. Q. Tang, *Int. J. Nanomed.*, 2021, **16**, 4197–4208.

9 K. Desale, K. Kuche and S. Jain, *Biomater. Sci.*, 2021, **9**, 1153–1188.

10 A. D. Frankel and C. O. Pabo, *Cell*, 1988, **55**, 1189–1193.

11 M. Green and P. M. Loewenstein, *Cell*, 1988, **55**, 1179–1188.

12 D. Derossi, A. H. Joliot, G. Chassaing and A. Prochiantz, *J. Biol. Chem.*, 1994, **269**, 10444–10450.

13 S. Futaki, T. Suzuki, W. Ohashi, T. Yagami, S. Tanaka, K. Ueda and Y. Sugiura, *J. Biol. Chem.*, 2001, **276**, 5836–5840.

14 Z. Lu, N. L. Truex, M. B. Melo, Y. Cheng, N. Li, D. J. Irvine and B. L. Pentelute, *ACS Cent. Sci.*, 2021, **7**, 365–378.

15 J. Narbona, L. Hernandez-Baraza, R. G. Gordo, L. Sanz and J. Lacadena, *Biomolecules*, 2023, **13**, 1042.

16 Z. Zhao, X. Liu, M. Hou, R. Zhou, F. Wu, J. Yan, W. Li, Y. Zheng, Q. Zhong, Y. Chen and L. Yin, *Adv. Mater.*, 2022, **34**, e2110560.

17 B. K. Jin, S. Odongo, M. Radwanska and S. Magez, *Int. J. Mol. Sci.*, 2023, **24**, 5994.

18 S. A. Kooijmans, C. G. Aleza, S. R. Roffler, W. W. van Solinge, P. Vader and R. M. Schiffelers, *J. Extracell. Vesicles*, 2016, **5**, 31053.

19 T. Nishiyama, K. Sugiura, K. Sugikawa, A. Ikeda and T. Mizuno, *Colloid Interface Sci.*, 2021, **40**, 100352.

20 K. Takahashi, T. Nishiyama, N. Umezawa, Y. Inoue, I. Akiba, T. Dewa, A. Ikeda and T. Mizuno, *Chem. Commun.*, 2024, **60**, 968–971.

21 M. Atabakhshi-Kashi, M. Carril, H. Mahdavi, W. J. Parak, C. Carrillo-Carrion and K. Khajeh, *Nanomaterials*, 2021, **11**, 1906.

22 A. Matucci, A. Vultaggio and R. Danesi, *Respir. Res.*, 2018, **19**, 154.

23 A. Gonzalez-Quintela, R. Alende, F. Gude, J. Campos, J. Rey, L. M. Meijide, C. Fernandez-Merino and C. Vidal, *Clin. Exp. Immunol.*, 2008, **151**, 42–50.

24 M. Sanchez-Navarro, M. Teixido and E. Giralt, *Nat. Chem.*, 2017, **9**, 727–728.

25 H. Son, J. Shin and J. Park, *RSC Adv.*, 2023, **13**, 9788–9799.

26 K. R. Schmitz, A. Bagchi, R. C. Roovers, P. M. van Bergen en Henegouwen and K. M. Ferguson, *Structure*, 2013, **21**, 1214–1224.

27 S. M. Rybak, S. K. Saxena, E. J. Ackerman and R. J. Youle, *J. Biol. Chem.*, 1991, **266**, 21202–21207.

28 X. Yang, Q. Tang, Y. Jiang, M. Zhang, M. Wang and L. Mao, *J. Am. Chem. Soc.*, 2019, **141**, 3782–3786.

29 R. Mout, M. Ray, T. Tay, K. Sasaki, G. Y. Tonga and V. M. Rotello, *ACS Nano*, 2017, **11**, 6416–6421.

30 A. Nagy, *Genesis*, 2000, **26**, 99–109.

31 H. Haigler, J. F. Ash, S. J. Singer and S. Cohen, *Proc. Natl. Acad. Sci. U. S. A.*, 1978, **75**, 3317–3321.

32 R. C. Roovers, T. Laeremans, L. Huang, S. De Taeye, A. J. Verkleij, H. Revets, H. J. de Haard and P. M. van Bergen en Henegouwen, *Cancer Immunol. Immunother.*, 2007, **56**, 303–317.

33 R. D. Qu and A. H. Huang, *J. Biol. Chem.*, 1990, **265**, 2238–2243.

34 J. T. Tzen, Y. K. Lai, K. L. Chan and A. H. Huang, *Plant Physiol.*, 1990, **94**, 1282–1289.

35 K. B. Vargo, R. Parthasarathy and D. A. Hammer, *Proc. Natl. Acad. Sci. U. S. A.*, 2012, **109**, 11657–11662.

36 I. Ghosh, A. D. Hamilton and L. Regan, *J. Am. Chem. Soc.*, 2000, **122**, 5658–5659.

37 N. Komatsu, K. Aoki, M. Yamada, H. Yukinaga, Y. Fujita, Y. Kamioka and M. Matsuda, *Mol. Biol. Cell*, 2011, **22**, 4647–4656.

38 K. Nishimura, T. Hosoi, T. Sunami, T. Toyota, M. Fujinami, K. Oguma, T. Matsuura, H. Suzuki and T. Yomo, *Langmuir*, 2009, **25**, 10439–10443.

39 R. Divine, H. V. Dang, G. Ueda, J. A. Fallas, I. Vulovic, W. Sheffler, S. Saini, Y. T. Zhao, I. X. Raj, P. A. Morawski, M. F. Jennewein, L. J. Homad, Y. H. Wan, M. R. Tooley, F. Seeger, A. Etemadi, M. L. Fahning, J. Lazarovits, A. Roederer, A. C. Walls, L. Stewart, M. Mazloomi, N. P. King, D. J. Campbell, A. T. McGuire, L. Stamatatos, H. Ruohola-Baker, J. Mathieu, D. Veesler and D. Baker, *Science*, 2021, **372**, eabd9994.

40 J. C. Charpentier and P. D. King, *Cell Commun. Signaling*, 2021, **19**, 92.

41 Y. S. Yang and T. E. Hughes, *BioTechniques*, 2001, **31**, 1036, 1038, 1040–1031.

42 N. Novak, C. Tepel, S. Koch, K. Brix, T. Bieber and S. Kraft, *J. Clin. Invest.*, 2003, **111**, 1047–1056.

43 Y. Z. Zhao, X. Q. Tian, M. Zhang, L. Cai, A. Ru, X. T. Shen, X. Jiang, R. R. Jin, L. Zheng, K. Hawkins, S. Charkrabarti, X. K. Li, Q. Lin, W. Z. Yu, S. Ge, C. T. Lu and H. L. Wong, *J. Controlled Release*, 2014, **186**, 22–31.